communications earth & environment

ARTICLE

https://doi.org/10.1038/s43247-022-00544-0 OPEN

Destabilization of carbon in tropical peatlands by enhanced weathering

Alexandra Klemme[1✉], Tim Rixen[2,3], Moritz Müller[4], Justus Notholt[1] & Thorsten Warneke[1]

Enhanced weathering is a carbon dioxide (CO_2) removal strategy that accelerates the CO_2 uptake and removal from the atmosphere by weathering via the dispersion of rock powder. Warm and humid conditions enhance weathering and among the suggested target areas for enhanced weathering are tropical peatlands. However, the effect of enhanced weathering on peatland carbon stocks is poorly understood. Here, we present estimates for the response of CO_2 emissions from tropical peat soils, rivers and coastal waters to changing soil acidity induced by enhanced weathering application. We estimate that the potential carbon uptake associated with enhanced weathering is reduced by 18–60% by land-based re-emission of CO_2 and is potentially offset completely by emissions from coastal waters. Our findings suggest that in contrast to the desired impact, enhanced weathering may destabilize the natural carbon cycle in tropical peatlands that act as important carbon sinks and protect against coastal erosion.

[1] Institute of Environmental Physics, University of Bremen, Otto-Hahn-Allee 1, 28359 Bremen, Germany. [2] Leibniz Center for Tropical Marine Research, Fahrenheitstr. 6, 28359 Bremen, Germany. [3] Institute of Geology, University of Hamburg, Bundesstr. 55, 20146 Hamburg, Germany. [4] Faculty of Engineering, Computing, and Science, Swinburne University of Technology Sarawak Campus, Jalan Simpang Tiga, 93350 Kuching, Sarawak, Malaysia. ✉email: aklemme@uni-bremen.de

The Paris climate agreement aims to limit the global average temperature rise to well below 2 °C with a target rise of less than 1.5 °C compared to pre-industrial times[1]. The Glasgow Climate Pact signaled progress in climate politics. Even with new pledges from several nations, the commitments are likely not enough to reach the 1.5 °C target of the Paris Agreement (ref. [2]). While reducing anthropogenic carbon dioxide (CO_2) emissions is a crucial strategy to mitigate global warming, it has become clear that atmospheric CO_2 removal techniques have to be deployed to meet this target[1,3]. One promising CO_2 removal technique is enhanced weathering (EW, ref. [4]). It accelerates the natural process of CO_2 uptake by weathering via the dispersion of rock powder over the land surface[5]. During weathering of the rock powder, atmospheric CO_2 is converted into carbonate that reacts with water to bicarbonate (HCO_3^-). It precipitates in soils and/or is washed out and transferred via rivers into the ocean[5]. In the ocean, this HCO_3^- supply counteracts acidification and potentially favors the CO_2 uptake from the atmosphere[5–7].

The tropics are key regions for EW. Model studies estimate a potential CO_2 uptake of 20–200 MgC km^{-2} year^{-1} with regional maxima of more than 1000 MgC km^{-2} year^{-1} (ref. [6,8,9]). Such high uptake is caused by warm and humid tropical climates accelerating the geochemical[6] and biologically enhanced[10] weathering. Preferred target areas for EW projects include tropical peatlands[8,9] of which 50% are located in Southeast Asia, mainly in the coastal flatlands of Sumatra and Borneo[11]. In their natural state, peatlands represent a carbon sink[12,13], stabilize the coast against erosion and flooding due to the formation of peat domes[14,15] and act as one of the last retreats for endangered wild life[16]. Since peat soils are acidic and agriculturally problematic, they have long been spared from cultivation. However, this has changed due to the ever-growing demand for palm oil and other agricultural products[17,18]. Today, more than 90% of the peatlands on Sumatra and Borneo are disturbed[19], with the consequence that the former CO_2 sinks have turned into CO_2 sources of global relevance[20]. Thus, peat soil conservation and restoration are considered as main measures to reduce CO_2 emissions and fulfill e.g., Indonesian climate pledges[21]. Combating climate change on the one side and increasing agricultural production on the other side represents a sustainability conflict that needs to be contextualized with EW as a CO_2 removal technique applied especially on actively worked croplands[9].

This study aims to estimate the response of CO_2 emissions from tropical peat soils, rivers, and coastal waters to EW application. For this, we investigate the impact of the EW-induced pH increase, caused by the enhanced HCO_3^- supply, on soil carbon mobilization in, and CO_2 emissions from tropical peatlands. We use known links between peat soil pH and soil carbon mobilization, develop a box model comprising river carbon dynamics, and apply coastal water mixing calculations to trace the fate of peat carbon and atmospheric CO_2 that is converted into HCO_3^- by weathering along the land-ocean continuum. Data obtained during measurement campaigns at Southeast Asian rivers[14,22,23] and the coastal ocean of Sumatra[24] were used to create and validate the carbon dynamics for the constructed river box model and to constrain realistic boundaries for the calculation of coastal water mixing. Based on these field data, we estimate the response of CO_2 emissions to EW application for a case study of Sumatra.

We find that the EW-induced pH increase potentially destabilizes tropical peat carbon reservoirs and enhances CO_2 emissions from soils, rivers, and coastal waters alike. This substantially reduces the CO_2 removal potential of EW in tropical peat regions.

Results and discussion

Increased soil CO_2 emissions and carbon leaching. Peat soil decomposition and the associated mobilization of peat carbon depend on the activity of the enzyme phenol oxidase[25], which is in turn strongly controlled by pH and oxygen (O_2, ref. [26]). Hence, a rise in pH levels would favor the decomposition of peat in soils and leached peat in peat-draining rivers[23,27]. Current estimates of the CO_2 uptake by EW do not include these processes[8,9] but peat soils are particularly vulnerable to pH as naturally occurring acidic conditions are one of the main preconditions for high carbon accumulation rates in peat soils and the resulting formation of peat[26].

We estimate the response of soil CO_2 emissions and dissolved organic carbon (DOC) leaching from soils to changes in pH caused by the realization of EW measures. According to current studies, a comparatively moderate basalt rock application of 1 kg m^{-2} year^{-1} over tropical regions increases the soil pH by 0.2–1.3 while causing a CO_2 uptake of 25–50 gC m^{-2} year^{-1} (refs. [8,9]). This pH increase in combination with known responses of peat carbon mobilization to changing pH values (ref. [28]) can be used to estimate CO_2 emissions and DOC leaching from peat soils. However, the EW estimates do not distinguish between peatlands and non-peatlands. Therefore, we discuss two cases: in case 1, we apply all estimates to tropical peat soils, assuming that the published EW uptake is representative for those soils. In case 2, we apply the published EW uptake to Sumatra, which is characterized by a peat coverage of ~15.6% (ref. [19]). In this case, the carbon mobilization is applied to Sumatra's peat soils only, assuming that the response of mineral soils is negligible in comparison.

For case 1, the EW-induced pH increase of 0.2–1.3 increases the carbon mobilization by 12–81 gC m^{-2} year^{-1} in form of CO_2 emissions and by 13–109 gC m^{-2} year^{-1} in form of DOC leaching (Fig. 1a). For the lower bound of the EW estimate (pH increase of 0.2) this carbon mobilization (≈25 gC m^{-2} year^{-1}) already compensates the CO_2 uptake by EW. For the upper bound (pH increase of 1.3) the carbon mobilization (≈190 gC m^{-2} year^{-1}) is considerably higher than the estimated CO_2 uptake by EW (Fig. 1a). This indicates that the application of EW on tropical peat soils could create a net CO_2 source to the atmosphere.

For case 2, we focus on the impact of carbon mobilization within Sumatra's peat soils on net CO_2 capture on Sumatra. While this approach might underestimate the carbon mobilization due to omitting of the response within mineral soils, the resulting mobilization of 2–13 gC m^{-2} year^{-1} in form of CO_2 emissions and 2–17 gC m^{-2} year^{-1} in form of DOC leaching implies that a large fraction of the CO_2 captured by EW (25–50 gC m^{-2} year^{-1}) is counteracted by carbon mobilization within peat areas (Fig. 1b).

The derived increase in CO_2 emissions is so far solely based on the pH-dependent impact of the phenol oxidase activity on peat decomposition[28]. It ignores the possibility of direct CO_2 re-emission due to the transformation of HCO_3^- to CO_2 under the acidic conditions in peat soils, as observed for liming experiments on plantations[29]. These experiments were conducted in a Finnish peat region and show similar carbonate application rates and pH changes to the EW estimates considered in our study. Those experiments revealed direct re-emission of 15% of the applied lime carbon. For the EW scenarios considered in this study, that would represent a re-emission of 3.8–7.5 gC m^{-2} year^{-1} from tropical peat soils. Based on this, 24–31% of the total increase in soil CO_2 emissions are caused by direct re-emission of the captured CO_2, while the remaining fraction is produced by enhanced soil decomposition.

Even though further studies will be needed to investigate this process in tropical peat, the same process will occur in peat-draining rivers. Hence, in contrast to assumptions that all EW captured CO_2 is transported to the ocean in the form of HCO_3^- (refs. [8,9]), the acidic conditions in peat-draining rivers could cause

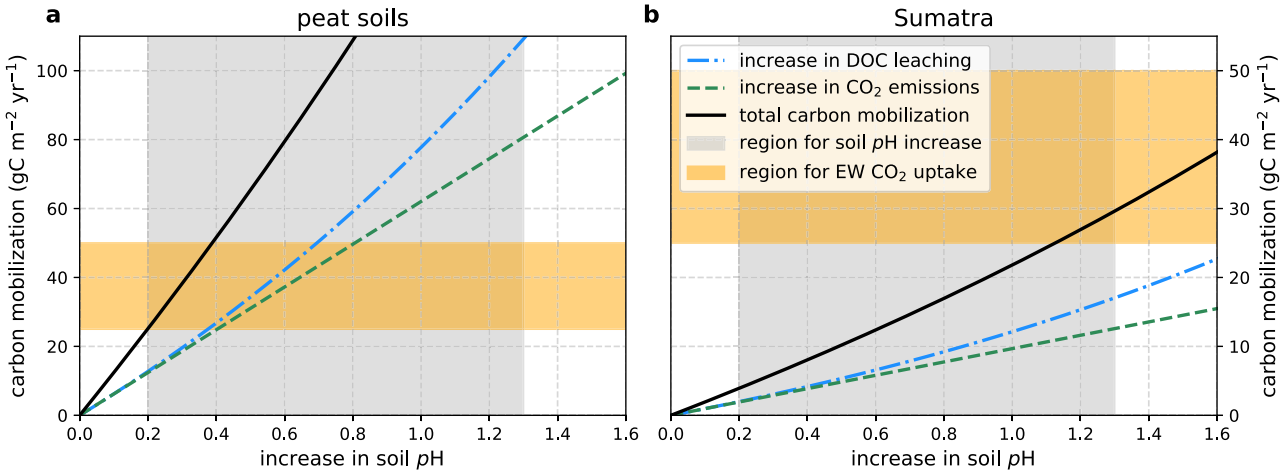

Fig. 1 Soil emission response to enhanced weathering. Carbon mobilization for basalt application of 1 kg m^{-2} year^{-1} on **a** peat soils (case 1) and **b** all of Sumatra's soils (case 2). Regions for the EW-induced soil pH increase and CO_2 uptake are estimated based on EW studies for tropical soils[8,9]. The pH dependences of CO_2 and DOC mobilization are based on data from a study on peat soils[28].

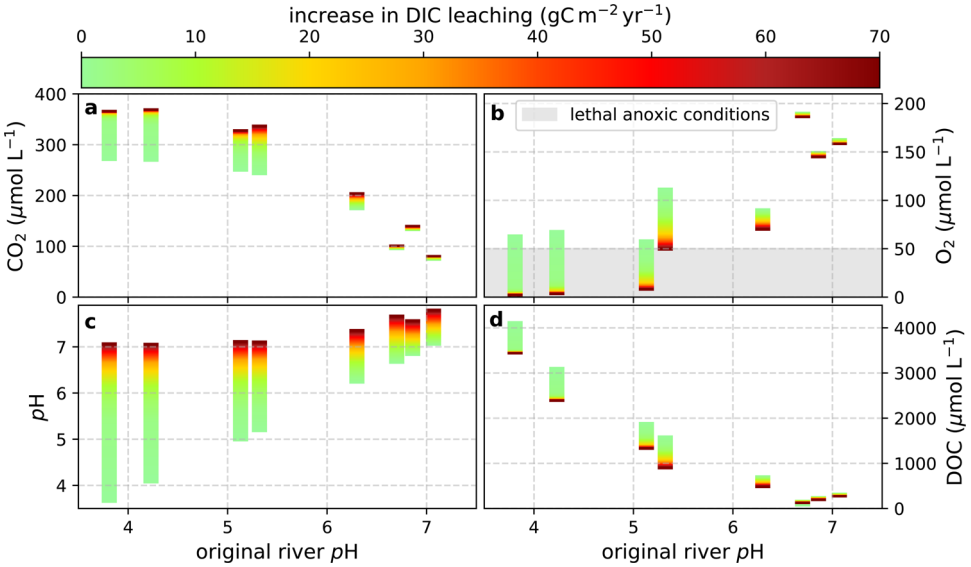

Fig. 2 Impact of enhanced weathering on river properties. Impact of enhanced DIC leaching on **a** CO_2 concentrations, **b** O_2 concentrations, **c** water pH, and **d** DOC concentrations in Southeast Asian rivers versus the original water pH. Colors indicate the response of parameters to enhancement in DIC leaching as e.g. caused by EW.

this HCO_3^- to transform into CO_2 and be re-emitted into the atmosphere. At the same time, the enhanced HCO_3^- supply could increase the river pH and thereby cause enhanced decomposition of the mobilized DOC, which again would enhance river CO_2 concentrations and emissions. To investigate the fate of leached DOC and dissolved inorganic carbon (DIC) in form of HCO_3^-, we developed and used a river box model.

River CO_2 emissions and oceanic carbon export. The impact of EW on river CO_2 emissions and the carbon export into the ocean was estimated based on the EW-induced increase in DIC and DOC leaching from soils using a river box model. This model includes pH and O_2-dependent decomposition processes, atmospheric gas exchange, and inorganic carbon dynamics. A detailed model description is provided in the methods. Reference runs of the river box model without increased carbon leaching (from here on called "natural runs", because they represent the conditions without EW application) were performed and validated using measured data from Southeast Asian rivers. These natural model runs result in average river CO_2 emissions from Sumatra of 3.5–10.1 TgC year^{-1}. For comparison, river emissions based on measured CO_2 concentrations and exchange coefficients result to 6.9 ± 1.7 TgC year^{-1}.

To quantify the impact of enhanced carbon leaching into the rivers, DIC and DOC leaching rates in the box model were increased. First, we consider only the increase in leaching of DIC while ignoring the enhanced carbon mobilization from peat soils. The increase in DIC (HCO_3^-) released during EW raises the river pH and reduces the CO_2 fraction in DIC. Rivers of high peat coverage (low pH) respond with a stronger pH increase than rivers of low peat coverage (high pH, Fig. 2c).

Decomposition rates in peat-draining rivers are limited by the acidic water[23]. Thus, the modeled pH increase induces enhanced in-river decomposition of DOC and therewith increases river CO_2 concentrations and emissions. Rivers with a strong pH increase (low original pH) also show a strong increase in CO_2 (Fig. 2a). This enhanced decomposition also causes a reduction of

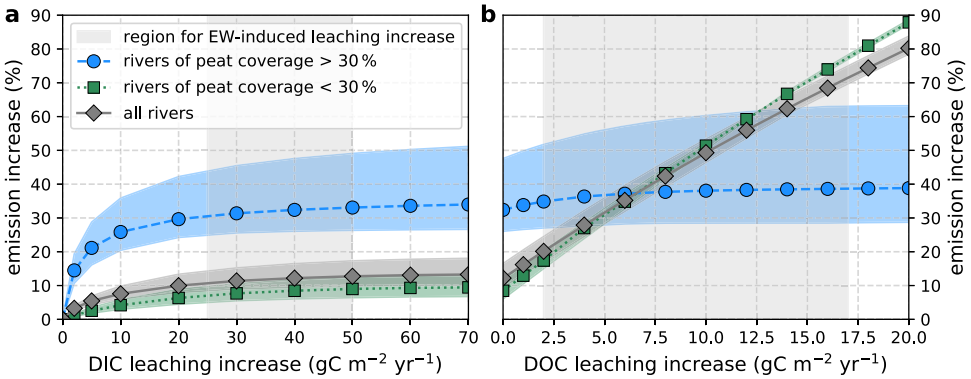

Fig. 3 River emission response to enhanced weathering. Response of river CO_2 emissions to EW as derived using the river box model. The emission increase was calculated for **a** increased DIC leaching and **b** increased DOC leaching in addition to an exemplary DIC leaching increase of 40 gC m^{-2} year^{-1}. Gray shaded areas indicate the estimated region for the EW-induced leaching increase. Shaded areas around the data points represent uncertainty based on best/worst case scenarios, as the errors of the decomposition parameters have been integrated throughout box model calculations.

DOC (Fig. 2b) and O_2 (Fig. 2d) in the rivers. Like the increase in CO_2, this decrease in DOC and O_2 concentrations is the strongest for rivers of low original pH, as those exhibit the strongest pH increase (Fig. 2c). For rivers with peat coverages higher than 50 % (pH < 5.2), O_2 concentrations decrease into the range of lethal anoxic conditions (Fig. 2d) and therewith limit in-river decomposition (refs. [23,30]) despite increased pH.

We compared the CO_2 increase caused directly by the HCO_3^- release during EW to the indirect CO_2 increase due to the pH mediated increase in DOC decomposition. We find that only 1–2% of the total increase in river DIC concentrations are directly caused by the carbonate input due to EW. The remaining fraction is caused by enhanced DOC decomposition.

In order to compare these river CO_2 emissions to the CO_2 uptake by EW, they were extrapolated to the area of Sumatra. Total river CO_2 emissions increase with increasing DIC leaching to the rivers (Fig. 3a) and stagnate for high leaching, as the impact of HCO_3^- on pH in the rivers becomes weaker (Fig. 2c) and O_2 depletion limits decomposition in rivers of high peat coverage (Fig. 2b). Due to the O_2 limitation, the stagnation is most prominent in rivers of high peat coverage (low original pH, Fig. 3a). The estimated DIC leaching increase for EW yields an increase in river CO_2 emission of 11–13%, whereby rivers of high peat coverage (>30%) show the strongest response (≈32%, Fig. 3a).

An additional increase in DOC leaching due to enhanced soil carbon mobilization considerably increases CO_2 emissions from rivers of low peat coverage (Fig. 3b). Its effect on rivers of high peat coverage is much smaller due to the depletion of O_2 (Fig. 2b) which hampers decomposition. Considering an exemplary increase in DIC leaching of 40 gC m^{-2} year^{-1} (which is within the range estimated for EW of 25–50 gC m^{-2} year^{-1}) and the increase in DOC leaching estimated for EW (2–17 gC m^{-2} year^{-1}), CO_2 emissions from Sumatra increase by 20–75% compared to the natural run (Fig. 3b). Deviations from the assumed DIC leaching of 40 gC m^{-2} year^{-1} result only in a small change in the functional dependence of CO_2 emissions on the DOC leaching increase and therefore in comparatively small changes in CO_2 emissions (Supplementary Fig. 2). Thus, the retrieved emission increase for enhanced DOC leaching of 40 gC m^{-2} year^{-1} seems to be representative of the estimated range.

The majority of riverine carbon that is not emitted to the atmosphere is transported to the ocean. This carbon export can be derived from modeled river DIC and DOC concentrations and river discharge. The natural box model run results in an oceanic carbon export of 7.5 TgC year^{-1} in form of DIC and 4.6 TgC year^{-1} in form of DOC. These exports are in the same order of magnitude as previous estimates for Sumatra[24]. Increased carbon leaching from soils substantially increases these oceanic carbon exports. At the increased DIC leaching rates estimated for EW, the oceanic DIC export increases by 16–32 TgC year^{-1} while the DOC export decreases by about 1 TgC year^{-1}. For the combined increase in DIC and DOC leaching, the oceanic DIC export increases by 11–33 TgC year^{-1}, and the oceanic DOC export changes by −1 to 4 TgC year^{-1} (Supplementary Fig. 3).

CO_2 emissions from estuaries and the coastal ocean. Emissions from river estuaries (<3 km distance from shore) and coastal oceans (3–67 km distance from shore) were calculated based on simple mixing calculations between river water and ocean water. Estuarine and coastal salinities were used to derive the ratio between river and ocean water, as described in the "Methods" section. Natural CO_2 emissions amount to 6.2 TgC year^{-1} from Sumatra's estuaries and 5.4 TgC year^{-1} from its coastal ocean, which agrees with recently stated estimates[24].

CO_2 emissions from these regions initially decrease for enhanced soil DIC leaching (Fig. 4a). This is caused mainly by the accompanying increase in water pH that shifts the DIC toward carbonates and favors carbonate dissolution in the ocean. At higher DIC leaching, the enhanced DOC decomposition in rivers causes an increased supply of inorganic carbon that overcompensates the uptake by the ocean. Estuary emissions increase above natural emissions for a DIC leaching increase of ≥5 gC m^{-2} year^{-1} (Fig. 4a). Further from the shore, in the coastal ocean, emissions are below natural for increased DIC leaching of up to 30 gC m^{-2} year^{-1} (Fig. 4a). Total emissions from these regions exceed natural emissions for a leaching increase of ≥12 gC m^{-2} year^{-1} (Fig. 4a). For the DIC leaching increase estimated for EW, emissions increase by 20–70%, which corresponds to a total increase of 2.4–8.2 TgC year^{-1} of which −0.3–1.4 TgC year^{-1} are emitted from the estuaries and 2.7–6.8 TgC year^{-1} are emitted from the coastal ocean.

An increase in DOC leaching in addition to the increased DIC leaching strongly increases coastal emissions (Fig. 4b). Considering an exemplary enhancement in DIC leaching of 40 gC m^{-2} year^{-1} in addition to the estimated increase in DOC leaching, total coastal CO_2 emissions increase by 70–380% compared to natural emissions (Fig. 4b). Variation of DIC leaching mainly affects coastal ocean emissions, while it shows little effect on estuary emissions (Supplementary Fig. 4). Considering the estimated EW induced increase in DIC and DOC leaching, the total coastal emissions increase by 8–44 TgC year^{-1}, of which

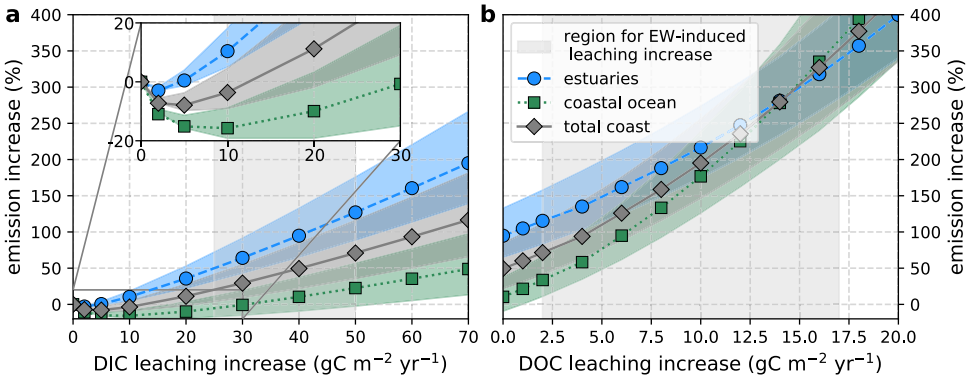

Fig. 4 Coastal emission response to enhanced weathering. Increase in coastal CO_2 emissions caused by **a** increased DIC leaching and **b** increased DOC leaching in addition to an exemplary DIC leaching increase of 40 gC m^{-2} year^{-1}. Gray shaded areas indicate the estimated region for the EW-induced increase in leaching. Shaded areas around the data points represent uncertainty based on best/worst case scenarios, as the errors of the decomposition parameters have been integrated throughout the box model and coastal mixing calculations.

2–25 TgC year^{-1} are emitted from the estuaries and 6–19 TgC year^{-1} are emitted from the coastal ocean.

Impact on the enhanced weathering CO_2 uptake for Sumatra. In order to quantify the response of tropical peat regions to EW, we compile the estimated CO_2 emissions from peat soils, peat-draining rivers, and coastal waters for a case study of Sumatra. For the sake of comparability, all estimates are presented in TgC year^{-1}. The estimated CO_2 uptake by EW in tropical regions of 25–50 gC m^{-2} year^{-1} (refs. [8,9]) yields a total uptake of 11.6–23.2 TgC year^{-1} over the land area of Sumatra. In the following, we summarize the results of our calculations and depict them in Fig. 5.

Enhanced CO_2 emissions from Sumatra's peat soils due to the EW-induced pH increase amount to 0.9–6.0 TgC year^{-1}, which represents 8–26% of the estimated EW CO_2 uptake for Sumatra. Additionally, soil carbon is mobilized via enhanced DOC leaching from soils. This DOC leaching mobilizes 0.9–7.9 TgC year^{-1}. Thus, the total carbon mobilization from Sumatra's soils amounts to 1.8–13.9 TgC year^{-1} (Fig. 5).

Captured CO_2 can be directly re-emitted to the atmosphere. Based on measurements in boreal peat soils, this re-emission amounts to ≈15% of the initial CO_2 uptake on peat soils (0.3–0.6 TgC year^{-1}). The rest of the captured CO_2 (11.3–22.6 TgC year^{-1}) is assumed to be leached into rivers in the form of HCO_3^-. This DIC leaching combined with the DOC leaching from soils increases emissions from Sumatra's rivers, estuaries, and coastal ocean by 0.9–7.4, 1.0–24.7 and 3.2–21.2 TgC year^{-1}, respectively (Fig. 5). Considering the CO_2 uptake by EW of 11.6–23.2 TgC year^{-1}, this implies that in a worst-case scenario the increase in carbon emissions resulting from EW application in peat regions could be substantially higher than the uptake by EW.

Since the CO_2 emissions strongly depend on the response of DOC leaching rates on EW and data, especially for tropical peat soils, are scarce, more research into the response of those leaching rates to increased soil decomposition is needed. Additionally, the estimates for coastal ocean CO_2 emissions are based on simplified mixing calculations and need to be viewed with caution.

Considering only the response of land-based CO_2 emissions from soils and rivers, enhanced emissions could reduce existing EW estimates by 18–60%, leaving a net CO_2 uptake of roughly 20 gC m^{-2} year^{-1}. This indicates that EW application in tropical peat regions could potentially create a carbon sink over land areas that would decrease tracked CO_2 emissions from specific countries while creating a substantial CO_2 source from coastal areas.

Conclusions

Our estimates show how pH changes due to EW application in tropical peat areas could impact CO_2 emissions from peat soils, peat-draining rivers, and the coastal ocean. We assumed moderate EW rock application rates of 1 kg basalt per year. Our results predict an increase in CO_2 emissions from peat soils of 16 to 89 gC m^{-2} year^{-1}, of which the majority (12–81 gC m^{-2} year^{-1}) is caused by increased peat decomposition. Those soil emissions alone could potentially be higher than the CO_2 uptake by EW on peat soils.

A case study for EW application on Sumatra was performed. We find that EW application would increase soil CO_2 emissions from Sumatra by 1.2–6.6 TgC year^{-1}. Enhanced carbon leaching into rivers due to increased soil DOC mobilization and leaching of the captured HCO_3^- additionally increases emissions from peat-draining rivers on Sumatra by 0.9–7.4 TgC year^{-1}. The majority of these enhanced CO_2 emissions (≈98%) are caused by increased DOC decomposition. Furthermore, changes in the in-river carbon dynamics impact the oceanic carbon export and cause an increase in CO_2 emissions from estuaries and the coastal ocean of 4.2–45.9 TgC year^{-1} that have the potential to completely counteract the CO_2 uptake by EW.

Overall, land-based carbon emissions from Sumatra's soils and rivers could reduce the net EW CO_2 uptake by 18–60%, of which 86–95% are caused by carbon mobilization and DOC decomposition. The inclusion of CO_2 emissions from Sumatra's coast increases the estimated re-emission to at least 50% with potentially more than 150% of the estimated CO_2 uptake. This indicates that EW application on Sumatra would create a carbon sink over land areas while it could create a substantial CO_2 source from the coast. These results show that the regional response of tropical peat areas has the potential to offset the CO_2 uptake by EW, and that these areas should accordingly be excluded from EW applications.

Though our estimates were derived based on a case study for Sumatra, the considered processes are globally valid for tropical peat soils and our results indicate the importance of soil type for the success of EW strategies. Thus, the response of different soil types to EW needs to be further studied before the application of EW.

Methods

Study area. Sumatra hosts more than 70,000 km^2 of peatlands[19], representing 15.6% of its surface area of 464,301 km^2 (ref. [31]). This is more than 30% of the whole Indonesian peat area and over 25% of the Southeast Asian peat area[20]. The development of peatlands is favored by Sumatra's warm and humid climate (Köppen classification Af), with mean annual precipitation of 2300 mm year^{-1} and

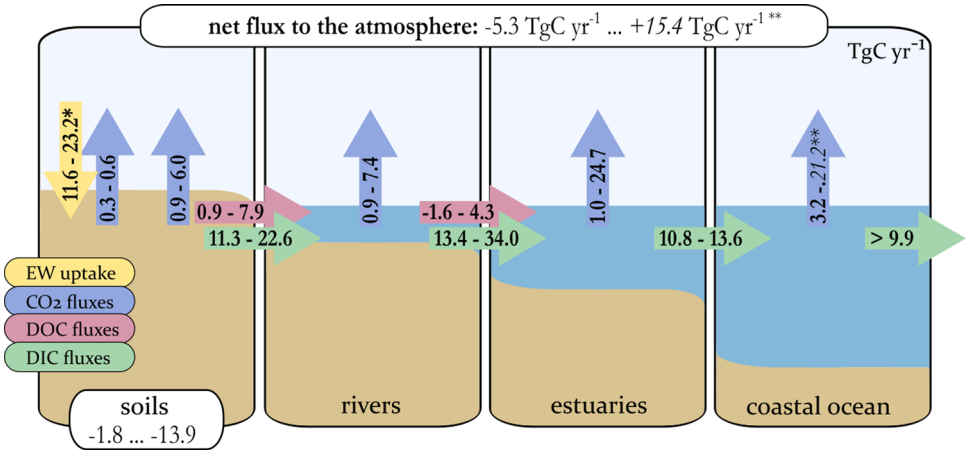

Fig. 5 Overview of changes in the carbon fluxes from Sumatra caused by enhanced weathering. Fluxes are presented in TgC year^{-1}. Blue values represent fluxes in form of CO_2, while red and green values represent DOC and DIC fluxes, respectively. Values in white boxes represent the net change in soils and the atmosphere. *The soil uptake is represented by published EW estimates[8,9]. **The upper bound of coastal ocean emissions is likely overestimated due to the simplified mixing calculations as explained in the methods.

a mean air temperature of 25.6 °C (ref. [32]). Peat regions on Sumatra are mainly located in flatlands along the east coast (Supplementary Fig. 1). Most Sumatran rivers originate in the Barisan Mountains and cut through those coastal peatlands before discharging into the Malacca Strait (Supplementary Fig. 1).

The aim of this study is to estimate the response of CO_2 emissions from Sumatra's soils, rivers and coastal regions to EW application. In the coastal regions, we thereby differentiate between the river estuaries and the coastal ocean. The areal extent of these categories, analogous to the study by Wit et al.[24], is defined by salinity with salinities ≤25 for estuaries and salinities within the range 25 to 32.8 for the coastal ocean. Based on the results by Wit et al.[24], these salinity values correspond to distances of ≈3 km and ≈67 km from shore and represent areas of 10,818 and 127,674 km^{-2}, respectively.

Data from rivers on Sumatra were obtained in a total of eight measurement campaigns conducted between 2004 and 2013 at the Siak, Indragiri, Musi and Batang Hari rivers[22]. Those data enabled us to construct a river box model and trace the fate of the carbon leached into rivers. The catchments of these rivers on Sumtra exhibit peat coverages between 4.0 and 25.9%. To also incorporate the impact of rivers with higher peat coverages, four rivers on Borneo (Sarawak, Malaysia) with peat coverages of up to 90.7% were included in addition to the Sumatran rivers. Those rivers include the Rajang, Simunjan, Sebuyau and Maludam (Supplementary Fig. 1). The data from Malaysian rivers were collected during six measurement campaigns between 2014 and 2017 (ref. [23]). Since all rivers drain tropical peat soils and are exposed to similar climatic conditions, they are considered representative for Southeast Asian peat-draining rivers and are handled equivalent in our calculations.

River parameters and catchment properties. River concentrations of CO_2, O_2 and DOC as well as water temperature, water pH, gas exchange coefficients (k_{600}), catchment sizes and peat coverages were determined as described in Klemme et al.[23] and are listed in Supplementary Table 1.

Stream surface areas were determined using stream widths based on the Global River Width from the Landsat (GRWL) Database[33]. For Maludam, Sebuyau and Simunjan, stream width was not available in GRWL, so it was calculated using the hydraulic equation by Raymond et al.[34]. River coverage was determined from the stream surface area divided by catchment size.

Precipitation data for the Maludam, Sebuyau and Simunjan catchments were provided by the Department of Irrigation and Drainage Sarawak. For the other catchments, precipitation was derived from the APHRODITE dataset[32]. For all catchments a 10-year average (2008–2017) was used.

River discharge was calculated from the difference between precipitation and evapotranspiration, multiplied by catchment area. The evapotranspiration was assumed to be 37.9% for moderately to severely disturbed catchments and 67.7% for undisturbed catchments as suggested by Moore et al.[35]. An evapotranspiration uncertainty of 15% is assumed, consistent with the calculations of Rixen et al.[14]. The value for undisturbed catchments was only used for the Maludam river. The total Sumatran discharge was calculated analogous to the river discharges with mean precipitation of 2300 mm year^{-1} (ref. [32]), evapotranspiration of 37.9% and an area of $A_{Sumatra} = 464{,}301$ km^2 (ref. [31]).

All derived catchment properties of the rivers, including CO_2 emissions, are listed in Supplementary Table 2.

River CO_2 emissions. River CO_2 emissions for the case study were derived by extrapolation of CO_2 fluxes from the individual rivers to the surface area of Sumatra. For this, individual river CO_2 fluxes were multiplied by the catchment's river coverages and weighed by catchment area. The resultant average CO_2 emissions per catchment area were then multiplied by the area of Sumatra.

Atmospheric CO_2 fluxes from individual rivers were calculated according to:

$$F_{CO_2} = k_{CO_2}(T) \cdot \left(K_{CO_2}(T) \cdot pCO_2^a - CO_2\right), \quad (1)$$

where pCO_2^a is the atmospheric partial pressure of CO_2 that for our calculations was assumed to be 400 µatm. K_{CO_2} describes the temperature dependent Henry coefficient, which was calculated according to Weiss[36]. k_{CO_2} is the exchange coefficient of CO_2 that was derived from k_{600} data according to:

$$k_{CO_2} = k_{600} \cdot \left(\frac{Sc_{CO_2}(T)}{600}\right)^{-n}, \quad (2)$$

with Sc_{CO_2} being the temperature dependant Schmidt number that was calculated according to Wanninkhof[37]. An exponent of $n = 2/3$ (valid for smooth surfaces and low wind speeds[38]) was used for the small Malaysian rivers (Maludam, Sebuyau and Simunjan) and an exponent of $n = 1/2$ (valid for rough surfaces[38]) for the bigger rivers. The atmospheric O_2 fluxes (F_{O_2}) were derived analogously with k_{O_2} calculated from Sc_{O_2} according to Wanninkhof[37] and Henry coefficients (K_{O_2}) calculated according to Weiss[39].

Gas exchange coefficients of rivers are poorly constrained and spatially as well as temporally extremely variable. Therefore, we only present the relative emission increase for individual rivers under the assumption that k_{CO_2} was not changed. Absolute river emissions presented for Sumatra were derived based on standardized exchange coefficients within the range of $k_{600} = 7$–20 cm h^{-1}, which covers measured exchange coefficients for Southeast Asian rivers[22,23].

Enhanced weathering estimates. We base estimates of CO_2 uptake, HCO_3^- formation and soil pH increase on studies by Taylor et al.[8] and Beerling et al.[9]. The estimates by Taylor et al.[8] are based on optimized EW scenarios for application of different rock types, rock application rates and application depths. In this study, we focus on EW with nutrient-rich basalt rocks. Those rocks exist in huge amounts and have been found to co-benefit crop production and soil health[9]. In tropical regions, the CO_2 uptake and pH increase for scenarios with basalt application by Taylor et al.[8] range from 50 to 300 gC m^{-2} year^{-1} and from 1.3 to 2.5, respectively.

Simulations by Beerling et al.[9] were performed for basalt application on cropland areas in different countries. For Indonesia, they resulted in formation of 2 to 3 molHCO_3^- m^{-2} year^{-1}, which correlate to a CO_2 uptake between 24 and 36 gC m^{-2} year^{-1}. Those estimates are lower than the ones Taylor et al.[8] stated for tropical weathering hotspot areas. They also result in a lower pH increase with less than 0.5 values for the region of Indonesia. Results for all considered EW scenarios are summarized in Supplementary Table 3.

Data in this study are based on the lower scale scenario by Taylor et al.[8] for application rates of 1 kg m^{-2} year^{-1} and an application depth of 10 cm over tropical weathering hotspot areas as well as on the scenario by Beerling et al.[9] for application of 4 kg m^{-2} year^{-1} over Indonesian cropland areas. Resulting CO_2 uptake and pH increase for those scenarios are 25–50 gC m^{-2} year^{-1} and 0.2–1.3, respectively.

Calculation of soil response to enhanced weathering. The response of soil CO_2 emissions and DOC leaching to EW was derived from the above-mentioned pH

increase of 0.2–1.3 in combination with correlations derived from published soil carbon mobilization and peat soil pH data[28]. Due to scarcity in data from tropical peat soils, the applied dependencies are based on data from temperate peat soils at 15 °C (ref. [28]). Comparison to data from temperate peat soils at 5 °C show that soils at 15 °C exhibit a slightly weaker response, which could indicate that the response at tropical temperatures is slightly weaker than estimated in this study.

Though Kang et al.[28] considered the response of soil CO_2 emissions to an increase in soil pH as nonsignificant within their study, it's impact cannot be neglected for a large-scale pH change as induced by EW. Their results suggest a correlation between pH and CO_2 mobilization that is approximately linear, whereat a pH increase of 1 value results in a CO_2 emission increase of 12 $gCO_2\ year^{-1}$ per kg of peat soil[28] (Supplementary Fig. 5). This CO_2–pH relation was applied to the upper soil layer (depth < 15 cm), where oxygen is available. A peat bulk density of $\rho = 0.127\ g\ cm^{-3}$ (ref. [40]) was used.

The response of DOC leaching was derived from a correlation between peat soil pH and DOC accumulation in peat porewater. DOC leaching is directly linked to the concentration of pore water DOC (ref. [41]). However, in contrast to the CO_2–pH correlation, the DOC–pH correlation is not linear. Instead, it is fairly well represented by a function that is $\sim 1.6^{\mathrm{pH}}$ (Supplementary Fig. 5). Thus, a value for the DOC leaching without EW is needed as reference to calculate the impact of pH changes on DOC leaching. This reference value was approximated by the sum of measured oceanic DOC export from Southeast Asian peat-draining rivers and in-river DOC loss by respiration[23] according to Eq. (3).

Additionally, we consider the direct re-emissions due to the transformation of HCO_3^- to CO_2 under the acidic conditions in peat soils. For tropical peatlands, no studies on the impact of direct re-emissions are available. However, Biasi et al.[29] performed measurements for a plantation on Finnish peatland. Their experiment was based on application of lime, amounting to 101 $gC\ m^{-2}$ in 2006. While this amount is by a factor of 2–4 higher than EW estimates considered in our study, the cold and dry climate in Finland that causes slower weathering rates than in tropical regions could compensate for that. The lime application caused an increase in soil pH of ~0.4, which is within the estimated range for EW. In their experiment, Biasi et al.[29] found annual lime-derived CO_2 emissions of 15.4 $gC\ m^{-2}\ year^{-1}$, representing ≈15% of the applied lime carbon.

Calculation of carbon leaching rates from soils. Natural DOC leaching rates from soils into rivers were approximated by the sum of oceanic DOC yield and DOC loss by respiration, which were calculated by the product of measured DOC concentration with the river discharge and with the respiration rate derived by Klemme et al.[23] (Eq. (4)), respectively:

$$\mathrm{DOC}_{\mathrm{leaching}} = \mathrm{DOC} \cdot Q + \mathrm{DOC} \cdot f_{\mathrm{dec}}(\mathrm{O}_2, \mathrm{pH}). \quad (3)$$

$$f_{\mathrm{dec}}(\mathrm{O}_2, \mathrm{pH}) = R \cdot \frac{\mathrm{O}_2}{K_{\mathrm{m}} + \mathrm{O}_2} \cdot \exp(\lambda \cdot (\mathrm{pH} - 7.5)) \quad (4)$$

Total DOC leaching from Sumatran soils was derived from the leaching rates calculated for the individual river catchments, weighed by catchment area and extrapolated to the total Sumatran area. The increase in DOC leaching that is caused by EW was derived based on the DOC–pH correlation described before.

Leaching rates of DIC from soils into rivers were approximated by the sum of oceanic DIC yield and DIC outgassing to the atmosphere minus DIC production by respiration:

$$\mathrm{DIC}_{\mathrm{leaching}} = \mathrm{DIC} \cdot Q + F_{\mathrm{CO}_2}\left(\mathrm{CO}_2, k_{\mathrm{CO}_2}, T\right) - \mathrm{DOC} \cdot f_{\mathrm{dec}}(\mathrm{O}_2, \mathrm{pH}). \quad (5)$$

Analogous to the total DOC leaching, the total DIC leaching from Sumatran soils was derived by DIC leaching into the individual rivers, weighed by the river catchments and extrapolated to the total Sumatran catchments. The increase in carbonate leaching rates that is caused by EW was approximated based on the assumption that the total CO_2 uptake by weathering is transformed to HCO_3^- and over time leached into rivers.

River box model for calculation of river response to enhanced weathering. To calculate the impact of changes in carbonate and DOC supply on river CO_2 emissions, a box model was constructed. The model simulates temporal changes in concentrations of DOC, DIC, carbonate alkalinity (CA), CO_2 and O_2 as well as in water pH. It includes decomposition processes, atmospheric exchange fluxes and reactions in the carbonate system as well as river input fluxes through leaching and discharge fluxes into the ocean.

For each model run, leaching rates of DOC, DIC, CA and O_2 as well as the water temperature, the salinity, the ratio between discharge and water volume (Q/V) and the ratio between exchange coefficients and water depth (k_{600}/d) were fixed to calculate equilibrium concentrations of the river parameters. Water temperatures of $T = 29$ °C and salinities of $S = 0.001$ were used for all rivers. For Q/V an average of all rivers ($(1.1 \pm 0.6) \cdot 10^{-6}\ s^{-1}$) was used and k_{600}/d was set to $(7.0 \pm 0.5) \cdot 10^{-6}\ s^{-1}$, as is consistent with results by Klemme et al.[23]. Natural leaching rates of DOC, DIC, CA and O_2 were derived according to Eqs. (3) and (5), $\mathrm{CA}_{\mathrm{leaching}} = \mathrm{CA} \cdot Q$ and $\mathrm{O}_{2,\mathrm{leaching}} = \mathrm{O}_2 \cdot Q - F_{\mathrm{O}_2}(\mathrm{O}_2, k_{\mathrm{O}_2}, T) + b \cdot \mathrm{DOC} \cdot f_{\mathrm{dec}}(\mathrm{O}_2, \mathrm{pH})$, with b being the fraction of O_2 that is consumed by decomposition compared to the CO_2 production (81%, ref. [23]). For model runs that simulate rivers impacted by EW, the increase in leaching was added to the natural leaching rates. Enhanced DOC leaching was added to the $\mathrm{DOC}_{\mathrm{leaching}}$ and enhanced DIC leaching was added to the $\mathrm{DIC}_{\mathrm{leaching}}$ and the $\mathrm{CA}_{\mathrm{leaching}}$.

For each model run, time steps of 10 min are iterated 52,560 times, amounting to 1 year of modeled concentrations. Generally new equilibrium states are reached after ~1 month (Supplementary Fig. 6).

Starting concentrations were set to the equilibrium concentrations derived from the natural river run (correlation to measured concentrations in the Supplementary Fig. 7). During each iteration, pH and CO_2 are calculated based on the current concentrations of DIC and CA according to Zeebe and Wolf-Gladrow[42]. Then, the changes in DIC, DOC, CA and O_2 concentrations due to the processes of leaching, decomposition, atmospheric exchange and discharge are calculated according to:

$$\begin{aligned}
\Delta\mathrm{DIC} &= Q/V \cdot \left(\mathrm{DIC}_{\mathrm{leaching}} - \mathrm{DIC}_{\mathrm{discharge}}\right) + \mathrm{DOC} \cdot f_{\mathrm{dec}}(\mathrm{O}_2, \mathrm{pH}) + \frac{1}{d} \cdot F_{\mathrm{CO}_2}(\mathrm{CO}_2, T, S) \\
\Delta\mathrm{DOC} &= Q/V \cdot \left(\mathrm{DOC}_{\mathrm{leaching}} - \mathrm{DOC}_{\mathrm{discharge}}\right) - \mathrm{DOC} \cdot f_{\mathrm{dec}}(\mathrm{O}_2, \mathrm{pH}) \\
\Delta\mathrm{CA} &= Q/V \cdot \left(\mathrm{CA}_{\mathrm{leaching}} - \mathrm{CA}_{\mathrm{discharge}}\right) \\
\Delta\mathrm{O}_2 &= Q/V \cdot \left(\mathrm{O}_{2-\mathrm{leaching}} - \mathrm{O}_{2-\mathrm{discharge}}\right) + b \cdot \mathrm{DOC} \cdot f_{\mathrm{dec}}(\mathrm{O}_2, \mathrm{pH}) + \frac{1}{d} \cdot F_{\mathrm{O}_2}(\mathrm{O}_2, T, S).
\end{aligned} \quad (6)$$

X_{leaching} and X_{river} are the concentrations of species X in the water input to the river and in the river water that discharges into the ocean, respectively. X_{river} are the current concentrations in the modeled river that the changes are applied to for each iteration. f_{dec} describes the O_2 and pH-dependent decomposition rate as derived by Klemme et al.[23] (Eq. (4)). F_{CO_2} and F_{O_2} describe the atmospheric fluxes of CO_2 and O_2, respectively. These fluxes were derived according to Eq. (1). Uncertainties for the derived concentrations were estimated from best/worst case runs of the box model based on variation of the respiration parameters (R, K_{m}, λ and b) within their uncertainties stated by Klemme et al.[23].

Oceanic yields from the individual rivers were calculated by multiplication of the derived concentrations with river discharges. The total oceanic DOC and DIC yields were derived from DOC and DIC concentrations in the individual rivers, weighed by river discharges and extrapolated to the total Sumatran discharge.

Calculation of estuarine and coastal response to enhanced weathering. In order to calculate the impact of coastal emissions on EW, coastal CO_2 concentrations were calculated for different oceanic carbon yields. We differentiate between emissions from the river estuaries and the coastal ocean. Analogous to Wit et al.[24], we define the areal extend of these categories by salinity with $S < 25$ for estuaries and $25 < S < 32.8$ for the coastal ocean. We assume conservative mixing of river water and ocean water for the estuaries and of estuarine and ocean water for the coastal ocean. It needs to be mentioned that our calculation assumes the river water to reach the coastal ocean unchanged, and thus does not account for the carbon loss caused by emissions from the estuaries. While this impact of estuarine CO_2 emissions might be negligible for the lower bound estimates of coastal ocean emissions, it could cause considerable overestimation in the upper bounds.

The mixing ratios between river water and ocean water in estuaries and the coastal ocean were derived based on salinity. As salinity increases linearly with the amount of salt in a specific water volume, the river water fraction within estuaries and the coastal ocean can be estimated from average salinities in the respective regions. The salinity within the estuaries ranges between 0 and 25 and its areal distribution is uneven[24]. Thus, the average estuarine salinity is not equivalent to the mean value between the lower and upper salinity bounds. The largest fraction of the estuarine area is located outside the river mouths with S > 10 and the increase in salinity per distance from shore weakens for greater distance from the river mouth[24]. Therefore, we use an average estuarine salinity of $S_{\mathrm{est}} \approx 20$. For the coastal ocean, where the salinity increase with distance from shore is fairly constant[24], the mean salinity of $S_{\mathrm{co}} \approx 28.9$ is used.

From known salinity of the ocean ($S_{\mathrm{ocean}} \approx 32.8$, ref. [43]) and the rivers ($S_{\mathrm{rive}} \approx 0.001$) fractions of river water in estuaries (a_{est}) and in the coastal ocean (a_{co}) can be derived according to:

$$\begin{aligned}
a_{\mathrm{est}} &= 1 - \frac{S_{\mathrm{est}} - S_{\mathrm{river}}}{S_{\mathrm{ocean}} - S_{\mathrm{river}}} \approx 39.4\% \\
a_{\mathrm{co}} &= 1 - \frac{S_{\mathrm{co}} - S_{\mathrm{river}}}{S_{\mathrm{ocean}} - S_{\mathrm{river}}} = \left(1 - \frac{S_{\mathrm{co}} - S_{\mathrm{est}}}{S_{\mathrm{ocean}} - S_{\mathrm{est}}}\right) \cdot a_{\mathrm{est}} \approx 12.4\%
\end{aligned} \quad (7)$$

Estuarine and coastal DIC and TA concentrations are derived according to:

$$\begin{aligned}
\mathrm{DIC}_{\mathrm{est/co}} &= a_{\mathrm{est/co}} \cdot \mathrm{DIC}_{\mathrm{river}} + (1 - a_{\mathrm{est/co}}) \cdot \mathrm{DIC}_{\mathrm{ocean}} \\
\mathrm{TA}_{\mathrm{est/co}} &= a_{\mathrm{est/co}} \cdot \mathrm{TA}_{\mathrm{river}} + (1 - a_{\mathrm{est/co}}) \cdot \mathrm{TA}_{\mathrm{ocean}}
\end{aligned} \quad (8)$$

Oceanic concentrations of DIC = 1900 $\mu mol\ l^{-1}$ and TA = 2200 $\mu mol\ l^{-1}$ (ref. [43]) are used and river concentrations are given by the equilibrium concentrations derived with the river box model. Additional assumptions for the

calculations are that the total river alkalinity is given by carbonate alkalinity ($TA_{discharge} = CA_{river}$) and that the whole DOC is oxidized when entering the estuaries ($DIC_{discharge} = DIC_{river} + DOC_{river}$).

From the calculated DIC and TA concentrations, estuarine and coastal CO_2 concentrations were derived by use of the CO2-SYS program[44,45]. This program was used for these coastal calculations of the carbonate system, as here the accurate calculations based on salinity are essential. For the earlier in-river box model calculations, where high concentrations of organic acids impair the results of the CO2-SYS program[46], the calculation according to Zeebe and Wolf-Gladrow[42] were used.

Atmospheric CO_2 fluxes were calculated based on the derived CO_2 concentrations and a coastal exchange coefficient of $k_{600} = 12\ cm\ h^{-1}$ (ref. [24]). To derive total emissions, these fluxes were multiplied by the estuarine and coastal ocean areas of $A_{est} = 10{,}818\ km^2$ and $A_{co} = 127{,}674\ km^2$ (ref. [24]).

Reporting summary. Further information on research design is available in the Nature Research Reporting Summary linked to this article.

Data availability

Observational data used to constrain the river box model are available at https://doi.org/10.5194/bg-19-2855-2022. Data generated and analyzed in the current study are available at https://doi.org/10.5281/zenodo.6961286.

Code availability

The river box model code (version 1.0.0) is available at https://doi.org/10.5281/zenodo.6961423. The CO2-SYS code (version 1.7.0) used for calculation of marine carbon dynamics is available at https://doi.org/10.5281/zenodo.4757055.

Received: 20 January 2022; Accepted: 31 August 2022;
Published online: 17 September 2022

References

1. de Coninck, H. et al. Sustainable development, poverty eradication and reducing inequalities. In: *Global Warming of 1.5 °C. An IPCC Special Report on the Impacts of Global Warming of 1.5 °C above Pre-industrial Levels and Related Global Greenhouse Gas Emission Pathways, in the Context of Strengthening the Global Response to the Threat of Climate Change, Sustainable Development, and Efforts to Eradicate Poverty*. https://www.ipcc.ch/sr15/ (2018).
2. O'Grady, C. The new climate pact is more ambitious. But hopes dim for limiting warming to 1.5 °C. *Science* **374**, 920–921 (2021).
3. Millar, R. J. et al. Emission budgets and pathways consistent with limiting warming to 1.5 °C. *Nat. Geosci.* **10**, 741–747 (2017).
4. Field, C. B. & Mach, K. J. Rightsizing carbon dioxide removal. *Science* **356**, 706–707 (2017).
5. Hartmann, J. et al. Enhanced chemical weathering as a geoengineering strategy to reduce atmospheric carbon dioxide, supply nutrients, and mitigate ocean acidification. *Rev. Geophys.* **51**, 113–149 (2013).
6. Strefler, J., Amann, T., Bauer, N., Kriegler, E. & Hartmann, J. Potential and costs of carbon dioxide removal by enhanced weathering of rocks, *Environ. Res. Lett.* **13** https://doi.org/10.1088/1748-9326/aaa9c4 (2018).
7. Köhler, P., Hartmann, J. & Wolf-Gladrow, D. A. Geoengineering potential of artificially enhanced silicate weathering of olivine. *Proc. Natl. Acad. Sci. USA* **107**, 20228–20233 (2010).
8. Taylor, L. L. et al. Enhanced weathering strategies for stabilizing climate and averting ocean acidification. *Nat. Clim. Change* **6**, 1758–6798 (2016).
9. Beerling, D. J. et al. Potential for large-scale CO_2 removal via enhanced rock weathering with croplands. *Nature* **583**, 242–248 (2020).
10. Taylor, L. et al. Biological weathering and the long-term carbon cycle: integrating mycorrhizal evolution and function into the current paradigm. *Geobiology* **7**, 171–191 (2009).
11. Page, S. E., Rieley, J. O. & Banks, C. J. Global and regional importance of the tropical peatland carbon pool. *Glob. Change Biol.* **17**, 798–818 (2011).
12. Sorensen, K. W. Indonesian peat swamp forests and their role as a carbon sink. *Chemosphere* **27**, 1065–1082 (1993).
13. Keller, J. Wetlands and the global carbon cycle: what might the simulated past tell us about the future? *New Phytol.* **192**, 789–792 (2011).
14. Rixen, T., Baum, A., Wit, F. & Samiaji, J. Carbon leaching from tropical peat soils and consequences for carbon balances, *Front. Earth Sci.* **4** https://doi.org/10.3389/feart.2016.00074 (2016).
15. Hoyt, A. M., Chaussard, E., Seppalainen, S. S. & Harvey, C. F. Widespread subsidence and carbon emissions across Southeast Asian peatlands. *Nat. Geosci.* **13**, 435–440 (2020).
16. Rixen, T. et al. *Science for the Protection of Indonesian Coastal Ecosystems (SPICE): Carbon Cycle in Tropical Peatlands and Coastal Seas* Ch. 4, 83–142 (Elsevier, 2022).
17. Posa, M. R. C. Peat swamp forest avifauna of Central Kalimantan, Indonesia: effects of habitat loss and degradation. *Biol. Conserv.* **144**, 2548–2556 (2011).
18. Zeng, Z. et al. Highland cropland expansion and forest loss in Southeast Asia in the twenty-first century. *Nat. Geosci.* **11**, 556–562 (2018).
19. Miettinen, J., Shi, C. & Liew, S. C. Land cover distribution in the peatlands of Peninsular Malaysia, Sumatra and Borneo in 2015 with changes since 1990. *Glob. Ecol. Conserv.* **6**, 67–78 (2016).
20. Hooijer, A. et al. Current and future CO_2 emissions from drained peatlands in Southeast Asia. *Biogeosciences* **7**, 1505–1514 (2010).
21. Roelfsema, M. et al. Are major economies on track to achieve their pledges for 2020? An assessment of domestic climate and energy policies. *Energy Policy* **67**, 781–796 (2014).
22. Wit, F. et al. The impact of disturbed peatlands on river outgassing in Southeast Asia. *Nat. Commun.* **6** https://doi.org/10.1038/ncomms10155 (2015).
23. Klemme, A. et al. pH regulation of CO_2 emissions from tropical rivers. *Biogeosciences* **19**, 2855–2880 (2022).
24. Wit, F., Rixen, T., Baum, A., Pranowo, W. S. & Hutahaean, A. A. The Invisible Carbon Footprint as a hidden impact of peatland degradation inducing marine carbonate dissolution in Sumatra, Indonesia. *Sci. Rep.* **8**, 2045–2322 (2018).
25. Freeman, C., Ostle, N. J., Fenner, N. & Kang, H. A. regulatory role for phenol oxidase during decomposition in peatlands. *Soil Biol. Biochem.* **36**, 1663–1667 (2004).
26. Pind, A., Freeman, C. & Lock, M. A. Enzymic degradation phenolic materials in peatlands. *Plant Soil* **159**, 227–231 (1994).
27. Williams, C. J., Shingara, E. A. & Yavitt, J. B. Phenol oxidase activity in peatlands in New York State: Response to summer drought and peat type. *Wetlands* **20**, 416–421 (2000).
28. Kang, H. et al. Biologically driven DOC release from peatlands during recovery from acidification. *Nat. Commun.* **9** https://doi.org/10.1038/s41467-018-06259-1 (2018).
29. Biasi, V. C. et al. Direct experimental evidence for the contribution of lime to CO_2 release from managed peat soil. *Soil Biol. Biochem.* **40**, 2660–2669 (2008).
30. Vaquer-Sunyer, R. & Duarte, C. M. Thresholds of hypoxia for marine biodiversity. *Proc. Natl. Acad. Sci. USA* **105**, 15452–15457 (2008).
31. Hooijer, A., Silvius, M., Wösten, H. & Page, S. PEAT-CO_2, assessment of CO_2 emissions from drained peatlands in SE Asia. *Delft Hydraulics report Q3943*. https://www.researchgate.net/publication/publication/ (2006).
32. Yatagai, A., Maeda, M., Khadgarai, S., Masuda, M. & Xie, P. End of the day (EOD) judgment for daily rain-gauge data. *Atmosphere* **11** https://doi.org/10.3390/atmos11080772 (2020).
33. Allen, G. H. & Pavelsky, T. M. Global extent of rivers and streams. *Science* **361**, 585–588 (2018).
34. Raymond, P. A. et al. Scaling the gas transfer velocity and hydraulic geometry in streams and small rivers. *Limnol. Oceanogr. Fluids Environ.* **2**, 41–53 (2012).
35. Moore, S. et al. Deep instability of deforested tropical peatlands revealed by fluvial organic carbon fluxes. *Nature* **493**, 660–663 (2013).
36. Weiss, R. F. Carbon dioxide in water and seawater: the solubility of a non-ideal gas. *Mar. Chem.* **2**, 203–215 (1974).
37. Wanninkhof, R. Relationship between wind speed and gas exchange over the ocean. *J. Geophys. Res. Oceans* **97**, 7373–7382 (1992).
38. Zappa, C. J. et al. Environmental turbulent mixing controls on air-water gas exchange in marine aquatic systems. *Geophys. Res. Lett.* **34** https://doi.org/10.1029/2006GL028790 (2007).
39. Weiss, R. The solubility of nitrogen, oxygen and argon in water and seawater. *Deep Sea Res. Oceanogr. Abstr.* **17**, 721–735 (1970).
40. Warren, M. W. et al. A cost-efficient method to assess carbon stocks in tropical peat soil. *Biogeosciences* 4477–4485 https://doi.org/10.5194/bg-9-4477-2012 (2012).
41. Worrall, F., Burt, T. P., Jaeban, R. Y., Warburton, J. & Shedden, R. Release of dissolved organic carbon from upland peat. *Hydrol. Process.* **16**, 3487–3504 (2002).
42. Zeebe, R. E. & Wolf-Gladrow, D. *CO_2 in Seawater: Equilibrium, Kinetics, Isotopes*, Ch. 1 (Elsevier Oceanography Series 65, Elsevier, 2001). https://epic.awi.de/id/eprint/4276/.
43. Schlitzer, R. Ocean Data View. https://odv.awi.de (2020).

44. Humphreys, M. P. et al. PyCO2SYS: marine carbonate system calculations in Python., Version 1.7.0, Zenodo. https://doi.org/10.5281/zenodo.4757055 (2021).
45. Lewis, E. & Wallace, D. W. R. Program Developed for CO_2 System Calculations., CDIAC, ESS-DIVE repository. Dataset https://doi.org/10.15485/1464255 (1998).
46. Lyu, L.-N. et al. A new software of calculating the pH values of coastal seawater: considering the effects of low molecular weight organic acids. *Mar. Chem.* **211**, 108–116 (2019).

Author contributions

A.K., T.R. and T.W. designed the study and analyzed the main results. M.M. and J.N. contributed data interpretation. A.K. led the writing of the paper. All authors discussed results and commented on the manuscript.

Funding

Open Access funding enabled and organized by Projekt DEAL.

Competing interests

The authors declare no competing interests.

Additional information

Supplementary information The online version contains supplementary material available at https://doi.org/10.1038/s43247-022-00544-0.

Correspondence and requests for materials should be addressed to Alexandra Klemme.

Peer review information *Communications Earth & Environment* thanks John Boyle and Kalu Davies for their contribution to the peer review of this work. Primary Handling Editors: Joshua Dean and Clare Davis. Peer reviewer reports are available.